

## ORIGINAL ARTICLE

WILEY

# Research on the dimensional accuracy of customized bone augmentation combined with 3D-printing individualized titanium mesh: A retrospective case series study

Linzhi Li MDS<sup>1</sup> | Chao Wang PhD<sup>1,2</sup> | Xian Li DDS<sup>1</sup> | Gang Fu PhD, DDS<sup>1</sup> |  
Dan Chen BA<sup>1</sup> | Yuanding Huang PhD, DDS<sup>1</sup> 

<sup>1</sup>Stomatological Hospital of Chongqing Medical University, Chongqing Key Laboratory of Oral Diseases and Biomedical Sciences, Chongqing Municipal Key Laboratory of Oral Biomedical Engineering of Higher Education, Chongqing, China

<sup>2</sup>Beijing Advanced Innovation Center for Biomedical Engineering, Beihang University, Beijing 100083, China

## Correspondence

Yuanding Huang, Stomatological Hospital of Chongqing Medical University, Chongqing Key Laboratory of Oral Diseases and Biomedical Sciences, Chongqing Municipal Key Laboratory of Oral Biomedical Engineering of Higher Education, Chongqing 401147, China.  
Email: huangyd@hospital.cqmu.edu.cn

## Funding information

National Natural Science Foundation of China, Grant/Award Numbers: 11872135, 12072055, 31100690; the Chongqing Science and Technology Bureau's new high-end R&D institution, Grant/Award Number: CSTC2018(C)XXYFJG0004; Program for Innovation Team Building at Institutions of Higher Education in Chongqing, Grant/Award Number: CXTDG201602006; National Science Foundation of China

## Abstract

**Background:** Few studies have focused on the dimensional accuracy of customized bone grafting by means of guided bone regeneration (GBR) with 3D-Printed Individual Titanium Mesh (3D-PITM).

**Purpose:** Digital technologies were applied to evaluate the dimensional accuracy of customized bone augmentation with 3D-PITM with a two-stage technique.

**Materials and methods:** Sixteen patients were included in this study. The CBCT data of post-GBR (immediate post-GBR) and post-implantation (immediate post-implant placement) were 3D reconstructed and compared with the pre-surgical planned bone augmentation. The dimensional differences were evaluated by superimposition using the Materialize 3-matic software.

**Results:** The superimposition analysis showed that the maximum deviations of contour between were 3.4 mm, and the average differences of the augmentation contour were  $0.5 \pm 0.4$  and  $0.6 \pm 0.5$  mm respectively. The planned volume of bone regeneration was approximately equal to the amount of regenerated bone present 6 to 9 months after the surgical procedure. On average, the vertical gain in bone height was about 0.5 mm less than planned. And, the horizontal bone gain on the straight buccal of the dental implants and 2 to 4 mm apical of the platform fell also about a 0.5 mm short on average. Statistically significant differences were observed between the augmented volume of virtual and post-GBR, and the horizontal bone gain of post-implantation on the level of 4 mm apical to the implant platform ( $P < .05$ ).

**Conclusions:** The dimensional accuracy of customized bone augmentation with the 3D-PITM approach needs further improvement and compared to other surgical approaches of bone augmentation.

## KEYWORDS

3D-printing individualized titanium mesh, computer aided design, customized bone augmentation, dimensional accuracy, guided bone generation

## 1 | INTRODUCTION

Rehabilitation of alveolar bone defects, caused by remodeling after tooth extraction, trauma, periodontal diseases, or congenital malformations, remains a major problem in implant dentistry. To gain a sufficient alveolar bone volume for successful and predictable dental implant placement, several surgical approaches have emerged over years.<sup>1,2</sup> As one of the reliable methods, GBR has become a major treatment option, due to its high predictability for the reconstruction of alveolar bone volume and contour.<sup>2,3</sup> The application of GBR for bone augmentation has been well documented, with the use of bone particulate grafts and barrier membranes, and demonstrated higher rates of success and lower complication rates.<sup>3-5</sup>

Despite the good clinical outcome, GBR with absorbable barrier is limited to small and moderate bone defects due to the poor space-making capacity and stability of collagen membranes.<sup>6,7</sup> When intended to augment severe horizontal defects or those with a vertical component, a much stable barrier, such as the prefabricated Ti-mesh (PFTM), could be necessary for bone reconstruction.<sup>4,8</sup> With its outstanding mechanical properties, PFTM has been used to maintain the space ensuring bone regeneration and resisting soft tissue collapse in challenging bone defects.<sup>9,10</sup> However, a high dehiscence rate (up to 80%) has been reported in many cases, which may attribute to the sharp edges and corners caused by presurgical shaping, bending and trimming.<sup>6,9,11,12</sup> In addition, considerable surgical skill is required to close the suture without stress.

As a potential alternative, 3D-printing individualized titanium mesh (3D-PITM) as reported by Ciocca (2011) has emerged, which is designed and manufactured in means of the CAD/SLM (computer-aided design/selective laser melting) techniques.<sup>13</sup> Biomechanical and animal researches have confirmed previously that 3D-PITM can provide excellent biocompatibility, adaptability, space-making capacity, adequate mechanical, and physical properties.<sup>14,15</sup> More importantly, in contrast to the traditional PFTM, the application of 3D-PITM showed lower mesh exposure rate (0%-33%), shorter operation time and lesser pain after GBR management.<sup>16-18</sup> Up to now, the existing literatures have revealed that the application of 3D-PITM for GBR can achieve satisfactory clinical efficacy and long-term stability with high GBR success rate and implant survival rate.<sup>16,18,19</sup>

However, whether the application of 3D-PITM, which is completed by precise preoperative design and manufacture, can achieve the predesigned bone contour and volume remain unclear. In fact, the predictability of GBR with 3D-PITM is of significant importance for evaluating the reconstruction of alveolar bone morphology and subsequent implant placement in augmented area. Therefore, it is pivotal to evaluate the dimensional accuracy of customized bone augmentation with 3D-PITM. However, almost all of the relevant reports only emphasizes on cross-sectional imaging measurement and clinical observation. Although Ottawa et al<sup>20</sup> has investigated the modeling accuracy of titanium products constructed with selective laser melting, the assessment of dimensional accuracy of customized bone grafting with 3D-PITM is still lack.

### What is known:

A large number of studies have shown that guided bone regeneration (GBR) technology has good predictability.

### What this study adds:

This study have evaluated the dimensional accuracy of customized bone augmentation with 3D-PITM through digital analysis, and found that the predictability of GBR with 3D-PITM approach needs further improvement.

To address this issue, a set of digital technologies was applied in this research, concluding 3D reconstruction of CBCT data, superimposition of digital models and 2D comparison of actual and virtual bone gain. Combining the measurements of 3D and 2D, the purpose of this retrospective study is to test the dimensional accuracy of customized bone augmentation combined with 3D-PITM within a two-stage technique in 16 patients with 25 implant sites. This study can help dentists to improve and optimize the preoperative design for future clinical application of 3D-printing individualized titanium mesh.

## 2 | MATERIAL AND METHODS

### 2.1 | Patients selection

From January 2018 to November 2019, a total of 32 patients had underwent GBR therapy with 3D-PITM. All patients were treated by the same surgical team in Oral Implantology Department, affiliated Stomatological Hospital of Chongqing Medical University, China. Sixteen patients with 25 implants meeting the following inclusion criteria were enrolled into this study:

1. Vertical alveolar defect or severe horizontal defects requiring bone augmentation before implant placement (class 4-5, Benic & Hammerle).<sup>3</sup>
2. Had undergone implant placement 6 ~ 9 months after GBR therapy with 3D-PITM in the first period.
3. With good physical health, willing to actively cooperate with the clinical study (Figure 1A).

Sixteen patients were excluded due to unavailable for regular follow-ups or without complete imaging data. Also, we excluded four patients who had to re-graft at re-entry due to complications of Ti-mesh (such as severe mesh exposure, infection, etc.). The retrospective evaluation was conducted on the basis of the principles embodied in the Declaration of Helsinki of 1975 as revised in 2000, and this study was approved by the ethics committee of Stomatological Hospital of Chongqing Medical University (2018LSno.7). Patients who met

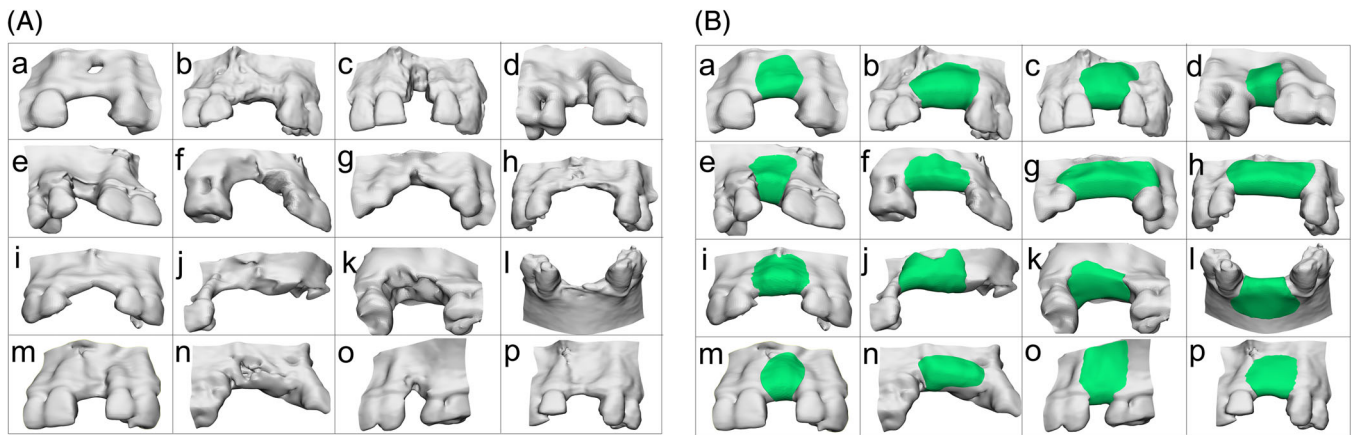


**FIGURE 1** Three-dimensional models of 16 patients. A, Different alveolar bone defects before GBR; B, Virtually reconstruction of alveolar bone

these criteria were informed of the study and signed an informed consent.

## 2.2 | Design and manufacture of 3D-PITM

A preoperative cone beam computer tomography (voxel size 0.4 mm; 85 kV; and approximately 35 mAs; CBCT, kava, Biberach, Germany) scanning was taken to obtain DICOM (Digital Imaging and Communications in Medicine) data of dual jaws of each patient, which were imported into Mimics Research software (Materialize, Leuven, Belgium) for 3D reconstruction and exported as STL files. The appreciate tooth model, implant model, and the reconstructed 3D model were transferred into 3-Matic software (Materialize, Leuven, Belgium) for simulation of restoration and implant placement. Each well-fitting dental element was positioned in respect to esthetic and functional parameters. And the virtual implant was planned with reference to the position of restoration. Considering the alveolar bone contour, soft tissue condition and the last but most important factor, the minimal bone tissue needed surrounding the implant, Geomagic software (Geomagic, North Carolina) was applied to reconstruct the alveolar bone defects virtually. After that, the simulated novel bone surface was over-thickened for about 1 mm using “move surface” operation in 3-matic software. The simulation of the alveolar bone reconstructions in 16 cases is shown in Figure 1B. Based on the virtual reconstruction of hard tissue, models of 3D-PITM for each case were designed by 3-Matic software with the thickness of 0.3 mm and uniform apertures of 2.0 mm diameter. The margins of the mesh should avoid damaging the important structures such as adjacent teeth, nerves, and blood vessels and be at least 2 mm away from these structures. Two or more retaining screw holes for the 3D-PITM were also planned cautiously in the apical or crestal margin of Ti-mesh with 2.0 mm diameter, avoiding to damage the root of adjacent teeth (Figure 2). At last, the completed model of 3D-PITM was imported into the 3D-printing machine (Lasercusing, concept laser GmbH, Germany) to produce the physical 3D-PITM with medical-grade Ti-alloy powder (Ti6Al4V, Dentarum, Germany). Subsequently, the final

products were checked and polished; after that, the thickness of 3D-PITM would be reduced to nearly 0.2 mm. Before the grafting in clinics, all 3D-PITM had been sterilized by high temperature and high pressure, reach the requirement of surveillance standard for cleaning, disinfection and sterilization (ISO 15883:2006).

## 2.3 | Clinical procedure and complications

After local infiltration anesthesia, a mid-crestal incision was made firstly and then, two relaxation incisions were added at the mesial or distal axial angle lines of neighboring teeth 1 ~ 3 units away from the edentulous region to achieve elasticity of the flap. Full-thickness mucoperiosteal flap were reflected and decortication was performed to enhance the revascularization in bone regeneration region. 3D-PITM had been tried on and adjusted to the optimal position according to the simulated location. On average 2.2 screw-holes were prepared subsequently through the designed apertures of Ti-mesh. An equal mixture (1:1) of particulate autogenous bone chips harvested with a ring shape bone-collecting drill and deproteinized bovine bone mineral (Bio-Oss, Geistlich Pharma AG, Wolhusen, Switzerland) was prepared, and as a whole mixed up with injectable platelet-rich-fibrin (i-PRF) for 10 minutes until it became into the namely “sticky bone” graft material. Right after all the preparation, half of the sticky bone graft was filled into the defect area, and the rest was loaded to the internal surface of 3D-PITM, which was immediately fitted to the preplanned position. Titanium fixing screws were put into the prepared holes and dual layer of resorbable collagen membrane (Bio-Gide, Geistlich Pharma AG, Wolhusen, Switzerland) and concentrated growth factor matrix were placed above the labial surface of Ti-mesh. Finally, a releasing incision was performed on the periosteum apically to the buccal flap and a more blunt dissection using the minime instrument was performed to further advance the flap. All flaps were closed with modified horizontal mattress suture, vertical mattress suture, and single sutures in the mid-crestal incision, gingival papilla, and releasing incisions, respectively.

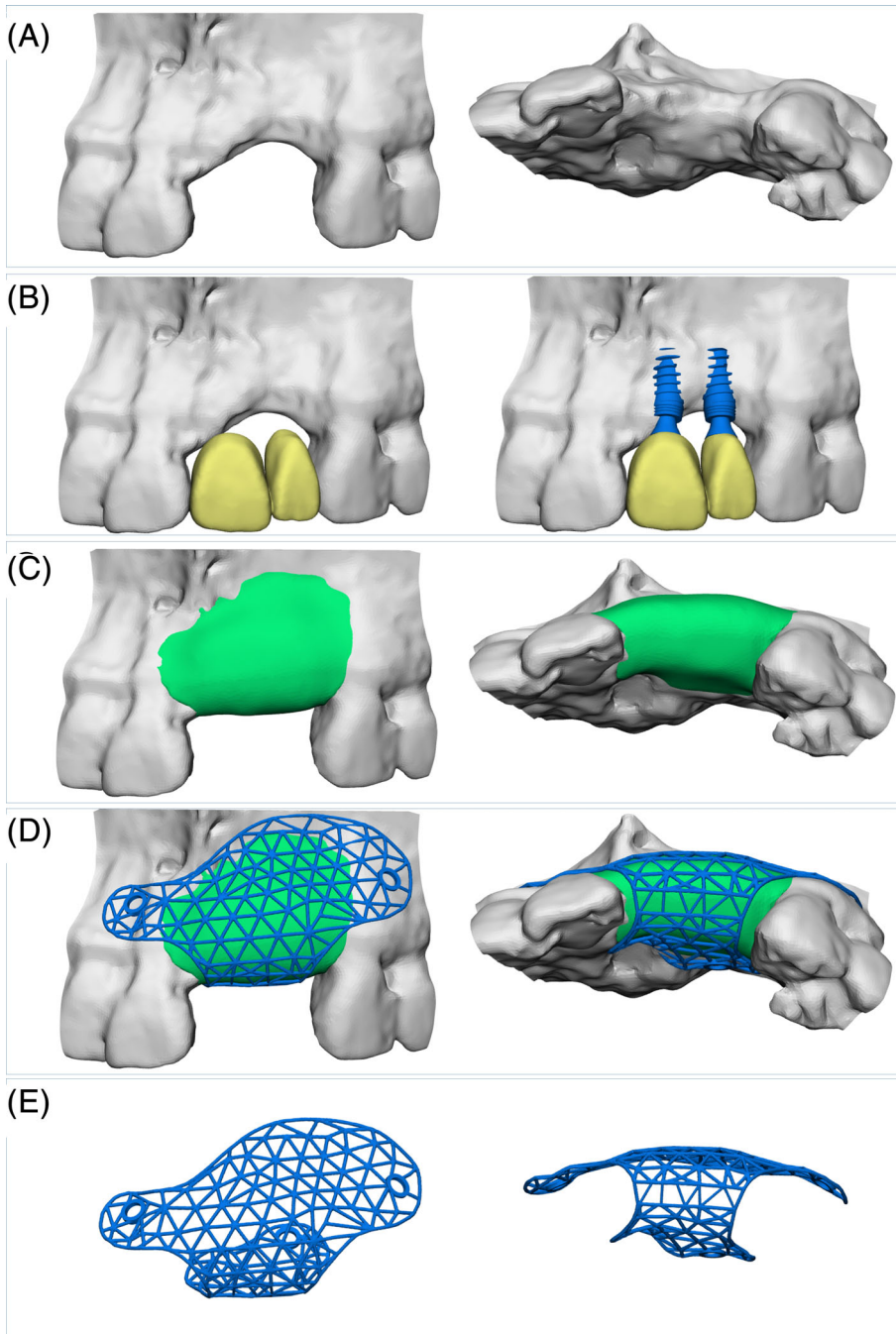


**FIGURE 2** The detailed design flowcharts of 3D-printing titanium mesh (3D-PITM). A, Three-dimensional reconstruction of alveolar bone before operation; B, Simulation of dentition restoration and implant placement; C, Reconstruction of the alveolar bone contour virtually (over-thickened for about 1 mm); D, Design of the 3D-PTIM on basis of the reconstructed bone contour; E, Complete the design of 3D-PTIM

Post-operative care consistent of 0.12% chlorhexidine mouth rinse, 2 g of amoxicillin (or 600 mg of clindamycin if allergic to amoxicillin) administered three times daily for 5 days. The single and mattress sutures were removed in 12 and 21 days, respectively. Patients were called back for following visits every 1 month after the surgery to investigate the healing and post-surgical complication. After 6 to 9 months of healing, CBCT scanning was performed and then reentry of the surgical sites was carried on with removal of the 3D-PITMs. During the operation, totally 25 implants were placed into the augmented alveolar bone. Four months later, another CBCT detection was completed and the final restorations were made (Figure 3).

### 3 | VERIFICATION OF DIMENSIONAL ACCURACY IN CUSTOMIZED BONE AUGMENTATION

#### 3.1 | Superimposition of the digital models

In order to verify the dimensional accuracy of customized bone grafting among virtual planning, the results of post-GBR (immediate post-GBR surgery) and post-implantation (immediate post-implant placement), DICOM data in every stage were imported into Mimics Research, and converted into 3D alveolar bone models with the same

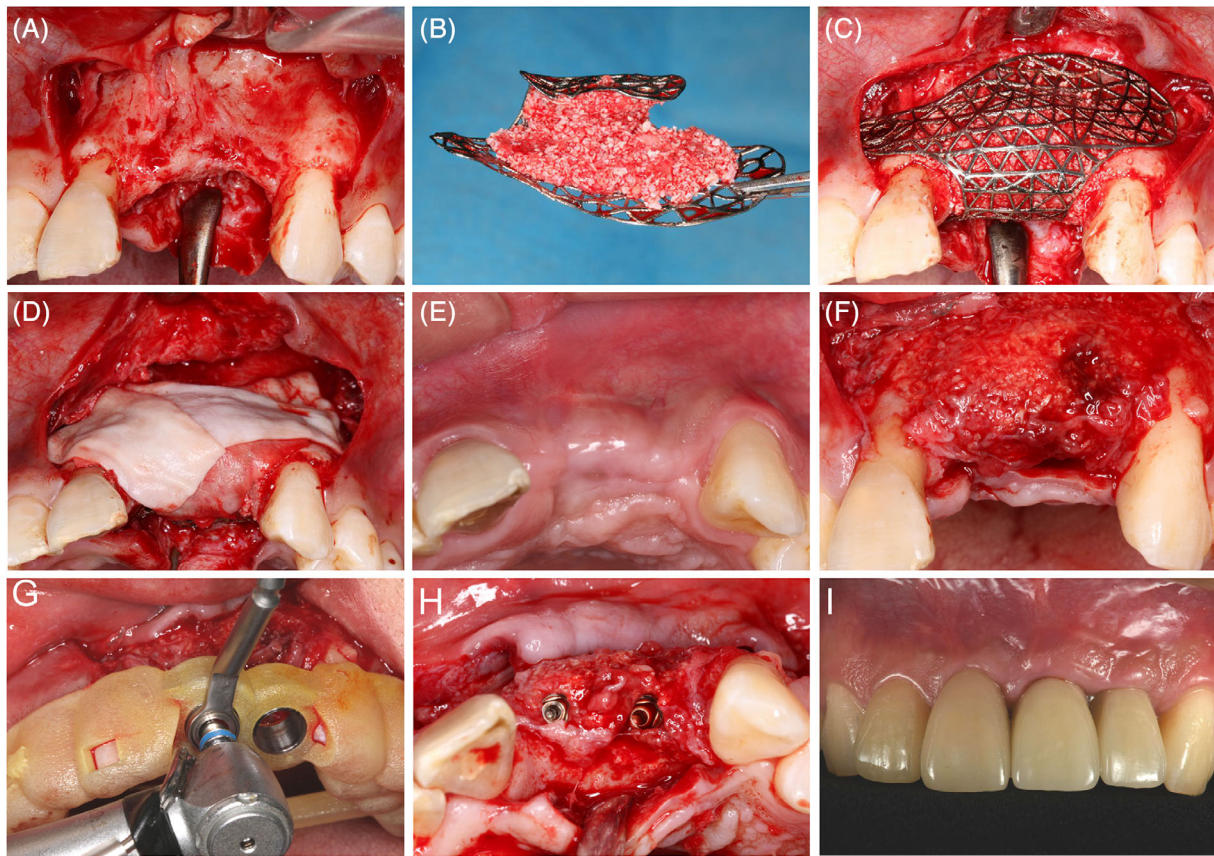


**FIGURE 3** Surgical procedure for GBR using 3D-PITM. A, Clinical appearance of the bone graft area displaying a mixed bone defect; B and C, 3D-PITM loaded with sticky bone was fitted in preplanned location; D, The mesh was covered by absorbable collagen membrane and concentrated growth factor membrane; E, Complications evaluation after surgery; F, Reconstructed bone after 6 to 9 months healing showed adequate vertical and horizontal bone augmentation were achieved; G, Implant placement was completed with a surgical template according to the actual bone amount; H, Implant installation; I, Prosthetic rehabilitation

threshold values. During the transformation of the immediate post-GBR model, the Ti-mesh profile was removed by adjusting the max threshold value, and its metal artifacts over the mesh were further reduced by noise reduction. After surface smoothing and deleting the internal structures, digital models of post-GBR (immediate post-GBR surgery) and post-implantation (immediate post-implant placement) were automatically aligned with the presurgical CAD designing model respectively via a registration tool in the Materialize 3-matic. For optimal alignment, as many as uniform and characteristic points of the reconstructed teeth were selected, such as the midpoint of the buccal surface or lingual/palate surface, the cusp point, the fovea, and so forth. Besides, a global registration with automatically selecting points was used to further overlap the three models.

After alignment, all three models (presurgical CAD designing model, model of immediate post-GBR and model of immediate post-implant placement) were trimmed into separated segments with similar distance (1 ~ 2 neighbor tooth) away from the borders of 3D-PITM or the corresponding GBR area with digital cutting tool, therefore to create coincident boundary among three models. Then, the dimensional differences among the three models were evaluated and calculated automatically by Materialize 3-matic in means of comparison analysis. The values were visually displayed with color maps,

which shows the positive or negative distance between different contours with colors. Meanwhile, the range of differences, the maximum and minimum distance were calculated and recorded (Figure 4).

### 3.2 | Digital evaluation of augmented contour

After the automatic comparison among three models, the augmentation contours covered by 3D-PITM was separated. The dimensional difference among the augmentation contour of preoperative contour, post-GBR contour and post-implantation contour were calculated in Table 2. Mean absolute distances as well as the SDs were also calculated and recorded (Table 2).

### 3.3 | Digital calculation of augmented volume

In the Materialize 3-matic software, the preoperative volume data of remaining alveolar bone was subtracted from the presurgical CAD model, the post-GBR model and the post-implantation model, respectively. Then, the augmented volumes of virtual planning and radiographic results were calculated in means of

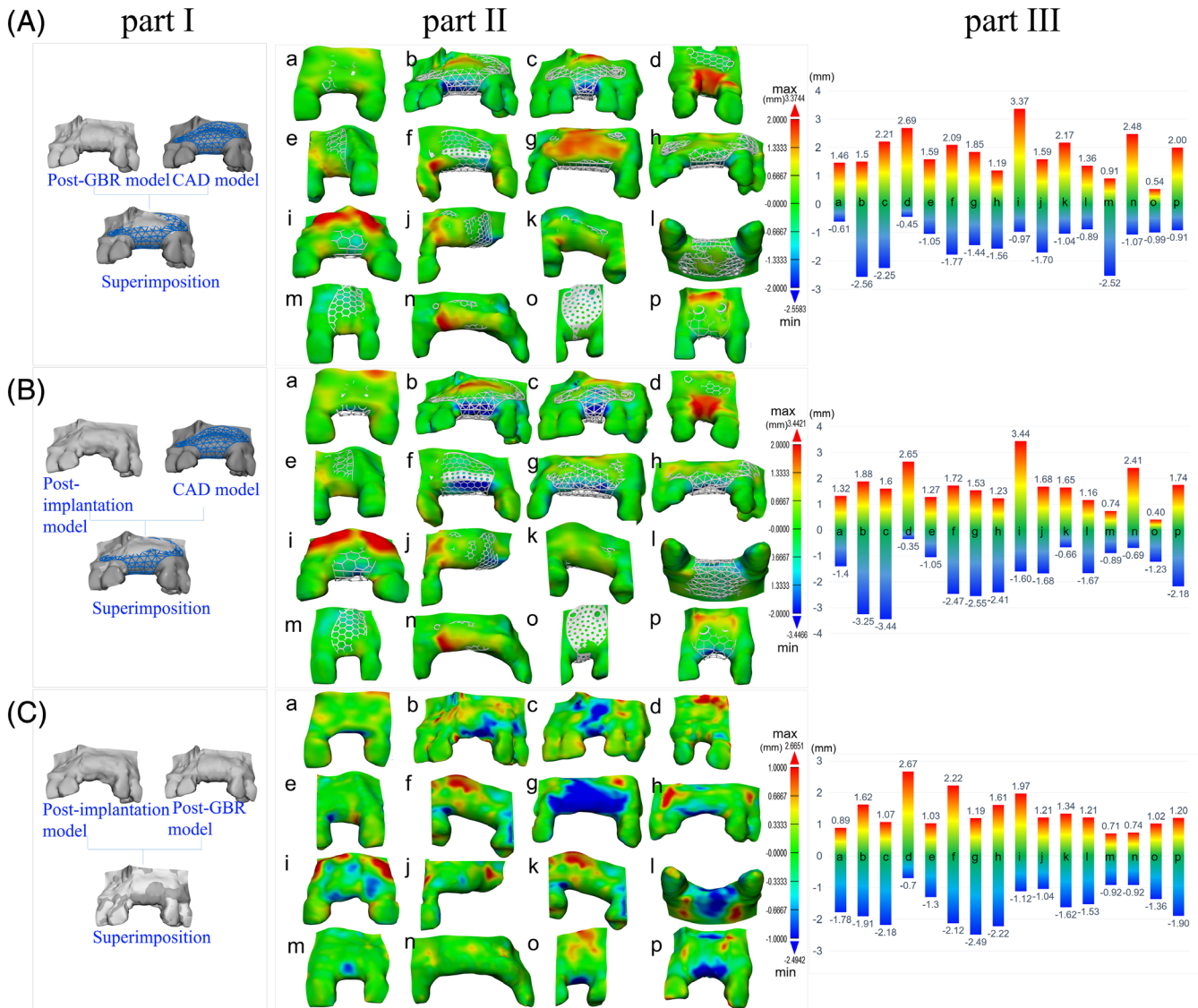


**FIGURE 4** Superimposition of the three digital models. A, The hard tissue dimensional difference between post-GBR models and CAD designing models. B, The hard tissue dimensional difference between post-implantation models and CAD designing models; C, The hard tissue dimensional difference between post-GBR models and post-implantation models. Part I, schematic illustration of three models overlapping each other; Part II, the differences were displayed with color maps. Blue surface shows the negative distance between the superimposed models, and red surface indicates the positive distance between them; Part III, the specific data of the maximum and minimum distance were calculated and shown in the column chart

automatic analysis. Volumetric difference of augmented bone among the three models was calculated and mean ± SD were used to describe the result.

### 3.4 | 2D digital measurement in cross-sections

Due to the integration of the bone grafts and the residual alveolar bone, it was difficult to distinguish the demarcation line between them. Therefore, in order to evaluate the augmented bone, all cases underwent a further digital approach for CBCT measurements as following protocol:

1. Preoperative model, CAD model and post-GBR model were superimposed with the post-implantation model in Materialize 3-matic as aforementioned. The combined models along with the CBCT data of post-implantation were imported into Mimics Research. Therefore, bony profile of four models were marked as red, yellow, green and blue lines respectively on the background of CBCT gray images in cross-sectional view.
2. The vertical augmentation of alveolar bone was evaluated along the central axis of the implant profile. The distance from the red line (the profile of residual bone) to the yellow line (the profile of CAD bone augmentation) was measured as the height of virtually bone gain (Hv), and that from the red line to the other two lines,

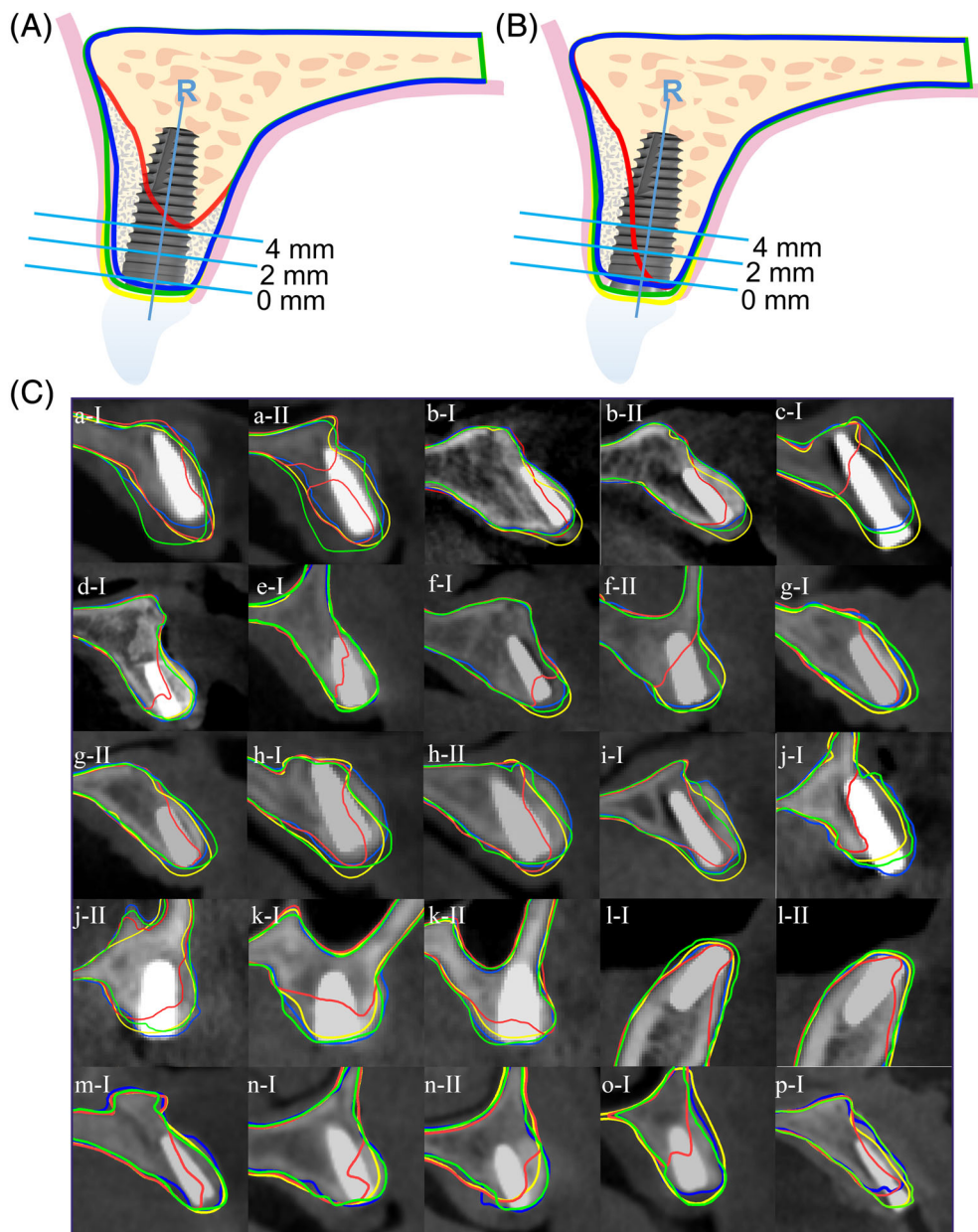


**FIGURE 5** The diagrammatic sketch illustrating the measurement of different bone levels. The central axis of the placed implant was marked as the reference line “R.” Red line: bony profile of residual bone; yellow line: bony profile of CAD bone augmentation; green line: bony profile after GBR; blue line: bony profile after implant placement. A, The vertical augmentation was measured along line “R,” the distance from the red line to the yellow line was measured as the height of virtually bone gain ( $H_v$ ), and that from the red line to the other two lines, the green line and the blue line, were measured as the actual height of bone graft ( $H_b$ ) and new bone ( $H_n$ ), respectively. Three lines which perpendicular to line “R” at levels of 0, 2, and 4 mm below the implant platform were intersected with bony profiles. When the perpendicular lines were not intersected with the red profile line, the width of virtually bone gain ( $T_v$ ), the actual width of bone graft ( $T_b$ ) and the actual width of new bone ( $T_n$ ) were the width of the yellow, green or blue profile in the perpendicular direction. B, When the perpendicular lines were intersected with the red profile line, the distance from the red line to the yellow line was measured as  $T_v$ , that from the red line to the green line was measured as  $T_b$ , and that from the red line to the blue line was measured as  $T_n$ . C, CBCT cross-sectional views along the central axis of the 20 implant sits after implant placement. The bony profile of four models was marked as red, yellow, green, and blue lines, respectively. And the measurements were conducted in these planes

the green line (the profile of bone augmentation after GBR) and the blue line (the profile of bone graft and basal bone after implant placement), were measured as the actual height of bone graft ( $H_b$ ) and new bone ( $H_n$ ), respectively.

3. The horizontal augmentation of alveolar bone, which was labeled as  $T_b$ ,  $T_n$ , and  $T_v$  in postoperative situations and CAD model, respectively, was measured in the similar way described upon. The central axis of the implant profile was regarded as a reference line,

perpendicular to which three lines at different levels such as 0, 2, and 4 mm apical to the platform of implant were intersected with the yellow (profile of CAD bone augmentation), green (the profile of bone augmentation after GBR) and blue line (the profile of bone graft and basal bone after implant placement), sometime even with the red line (the profile of residual bone). Two individual situations might occur in different sites: (a) When the perpendicular lines were not intersected with the red profile line,  $T_v$ ,  $T_b$ , and  $T_n$  were the width of the yellow, green or blue profile in the perpendicular direction of the cross-sectional views (Figure 5A). (b) When the perpendicular lines were intersected with the red profile line, the distance from the red line to the yellow line was measured as  $T_v$ , that from the red line to the green line was measured as  $T_b$ , and that from the red line to the blue line was measured as  $T_n$  (Figure 5B). The horizontal measurements were conducted at three different levels (0, 2, and 4 mm apical to the platform of implant profile) and each of them was repeated for three times by the same investigator (Figure 5C). A mean value for each patient was calculated and mean  $\pm$  SD were used to describe the result.

## 4 | DIGITAL MEASUREMENT OF THE BONE RESORPTION

To determine the changes of bone augmentation, CBCT was taken 10 to 18 months after GBR and 3D reconstructed in Mimics Research (the fourth model). The reconstructed model was superimposed with the post-implantation model (immediate after implant placement) in Materialize 3-matic software as aforementioned. For volume changes, the reconstructed model was subtracted from the post-implantation model, and the volume value was calculated by automatic analysis in the Materialize 3-matic software. For vertical and horizontal resorption, the reconstructed model along with the CBCT data of post-implantation was imported into Mimics Research. The distance between the two bone profiles along the central axis of implant was measured as the vertical bone resorption. Besides, three reference lines (0, 2, and 4 mm apically from the top of the implants) perpendicular to the central axis of implant were chosen to standardize the horizontal bone changes measurement. The distance between the two profiles at the three reference lines were measured as the horizontal resorption of the labial bone.

## 5 | STATISTICAL ANALYSIS

All statistical analysis was performed using SPSS (IBM SPSS Statistics version 20.0, IBM, Armonk, New York). The outcome of color mapping was represented with bar charts and the data were reported with ranges, means, and SD. Therefore, descriptive statistical analysis was used to display the results of the superimposition of the digital models and the results of bone resorption. A paired T test was conducted on a patient basis to assess the difference of bone gain (augmented bone

volumes, vertical bone gain and horizontal bone gain of 0, 2, and 4 mm apical to the implant platform) between virtual designing and actual situation (post-GBR and post-implantation). Means, SDs, and 95% confidence intervals (CIs) were calculated for the accuracy of the bone gains. All statistical comparisons were conducted at the .05 level of significance.

## 6 | RESULTS

### 6.1 | Patient profile

In this study, 16 patients including 9 males and 7 females, who had underwent GBR with 3D-PITM and secondary implant placement in 16 defect sites were enrolled into analysis. The mean age of patients at the time of GBR was  $32.5 \pm 12.4$  years (in the range of 18 ~ 55 years). All patients were non-smokers without periodontal diseases. Among them, 14 patients presented a thick gingival morphotype and only 2 patients presented a thin gingival morphotype. Of the 16 bone defects, 11 defect sites were located in the pre-maxilla, four defect sites in the posterior maxilla, and one defect in the anterior mandible. The range of the GBR sites was from 1 ~ 5 teeth (average 2.3 teeth). Eight out of 16 patients had combined alveolar defects, 5 with vertical defects, and 3 with severe horizontal defects. All patients' characteristics are summarized in Table 1.

### 6.2 | Clinical and radiographic outcomes

The soft tissues healing of 12 patients (75%) out of 16 was uneventful during 6 ~ 9 months follow-up after GBR with 3D-PITM, while dehiscence was observed in 4 patients (25%). Among the 4 cases, three occurred on the alveolar crest and presented the exposure of 3D-PITM on the seventh, 21th and 28th day after GBR, respectively, and the other one was observed on the palatal side on the 30th day but without Ti-mesh exposure. No signs of infection were identified in all four cases and no special treatment was conducted except irrigating with 0.12% chlorhexidine mouthwash twice per day until healing of soft tissue. After 6 ~ 9 months, all GBR sites were re-entered to remove the screws and 3D-PITMs, under which layers of fibrous tissue called as pseudo-periosteum<sup>21</sup> by authors had been detected. The

**TABLE 1** Characteristics of selected patients

Mean age (range)	32.5 $\pm$ 12.4 years (18-55)
Female/male (n = 12)	7/9
Smoker	0
Periodontal disease	0
Gingival morphotype (thick/thin)	14/2
Maxillary/mandibular cases	15/1
Mean missing teeth sites (range)	2.25 $\pm$ 1.18 teeth (1-5)
Mixed/vertical/horizontal bone defects	8/5/3

thickness of pseudo-periosteum was measured using a UNC-15 periodontal probe, featuring a 1 mm graduated scale, at four sites (mesial, distal, buccal, and crestal) under Ti-mesh. And the results showed 11 patients (68.75%) were under 1 mm, 4 patients (25%) were between 1 and 2 mm, and only 1 patient (6.3%) was over 2 mm. In the process of removing the 3D-PITM, part of the pseudo-periosteum infiltrated in the pores of the 3D-PITM was removed simultaneously. The remaining pseudo-periosteum, which adhered to the new bone, was removed using an elevator by blunt separation (Figure 6).

After removal of the *pseudo-periosteum*, healthy and revascularized new bone was presented with sufficient volume for

implant placement in all augmentation sites. Based on the actual bone volume and contour, we made some fine adjustments on the position of implant. With aids of CAD-CAM surgical guided plates, a total of 25 implants were placed in the optimal sites and axis, with an average insertion torque value of  $42.00 \pm 7.36$  Ncm and an ISQ value of  $63.32 \pm 4.88$ . According to the post-implantation CBCT evaluation, the average vertical bone gain on a patient basis was  $3.55 \pm 3.74$  mm and the horizontal average bone gain was  $4.06 \pm 2.37$ ,  $5.58 \pm 2.65$ , and  $5.26 \pm 2.33$  mm at levels of 0, 2, and 4 mm below the implant platform. The mean bone volume gained was  $634.01 \pm 281.85$  mm<sup>3</sup> (Table 3).

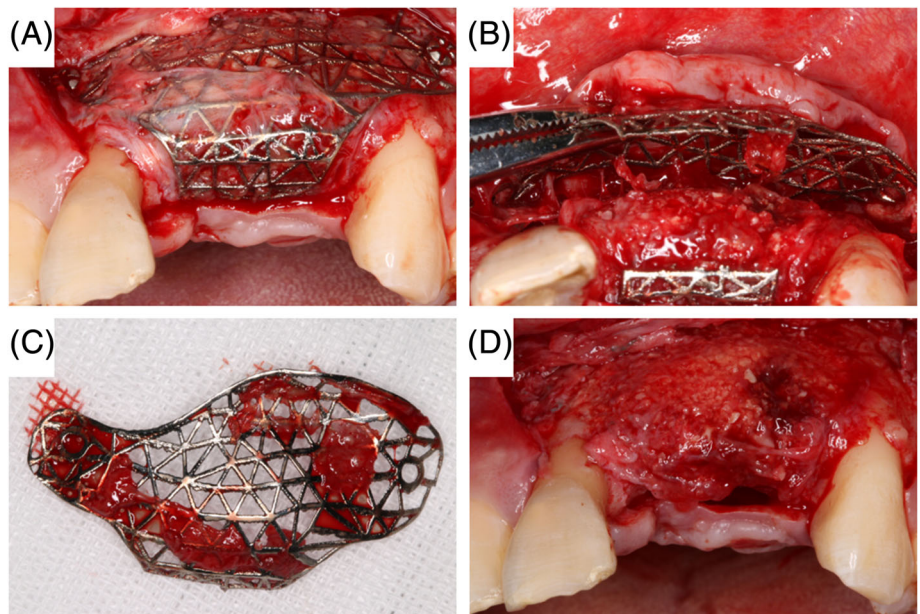


**FIGURE 6** The removal of 3D-PITM and the pseudo-periosteum. A, part of the pseudo-periosteum infiltrated in the pores of the 3D-PITM and closely connected to it. B, when removing the 3D-PITM, part of it was removed. C, Removed 3D-PITM and part of pseudo-periosteum. D, The remaining incomplete pseudo-periosteum adhered to the new bone

**TABLE 2** Descriptive analysis of the distance among the augmentation contour (the area covered by 3D-PITM) of preoperative contour, post-GBR contour and post-implantation contour after superimposition of three models (post-GBR models, post-implantation models and presurgical CAD designing models) using Materialize 3-matic software

A. The distance between the augmentation contours of post-GBR contour and preoperative contours				
	Min (negative)	Max (positive)	Mean absolute value	SD
Mean (mm)	-1.36	1.81	0.51	0.42
SD (mm)	0.65	0.70	0.17	0.17
B. The distance between the augmentation contour of post-implantation contours and preoperative contours				
	Min (negative)	Max (positive)	Mean absolute value	SD
Mean (mm)	-1.72	1.65	0.59	0.47
SD (mm)	0.92	0.51	0.19	0.18
C. The distance between the augmentation contour of post-GBR contours and post-implantation contours				
	Min (negative)	Max (positive)	Mean absolute value	SD
Mean (mm)	-1.57	1.36	0.39	0.33
SD (mm)	0.54	0.54	0.17	0.12

Abbreviations: Min, minimum; Max, maximum.

**TABLE 3** Paired t tests showed mean deviation between post-GBR model (immediate post-GBR surgery), post-implantation model (immediate post-implant placement), and presurgical CAD designing model

	CAD vs Post-GBR			CAD vs Post-implantation					
	CAD (Mean ± SD)	Post-GBR (Mean ± SD)	Difference (Mean ± SD)	95% CI (difference)	P-value	Post-implantation (Mean ± SD)	Difference (Mean ± SD)	95% CI (difference)	P-value
Gained bone volume (mm <sup>3</sup> )	636.20 ± 341.18	759.60 ± 362.43	-123.40 ± 136.62	-196.20~50.60	0.003	634.01 ± 281.85	2.18 ± 156.09	-80.99~85.36	.956
Gained bone height (mm)	4.11 ± 3.97	3.90 ± 3.70	0.22 ± 1.00	-0.32~0.75	0.404	3.55 ± 3.74	0.56 ± 1.35	-0.16~1.28	.118
Gained bone width (mm)	4.02 ± 2.86	4.34 ± 2.54	-0.33 ± 1.39	-1.07~0.41	0.361	4.06 ± 2.37	-0.04 ± 1.96	-1.09~1.00	.929
	5.21 ± 2.77	5.62 ± 2.75	-0.42 ± 1.09	-1.00~0.17	0.149	5.58 ± 2.65	-0.37 ± 1.02	-0.91~0.18	.172
	4.75 ± 2.79	5.01 ± 2.25	-0.26 ± 0.97	-0.78~0.25	0.298	5.26 ± 2.33	-0.51 ± 0.79	-0.93~0.09	.022

Note: Statistically significant difference exists between the augmented volume of virtual and post-GBR, and the horizontal bone gain of post-implantation on the level of 4 mm apical to the implant platform ( $P < .05$ ). Gained bone volume: the volume obtained after preoperative model subtracted from the CAD model, the post-GBR model and the post-implantation model respectively. Gained bone height: the distance of bone profiles between preoperative model and the three models respectively along the central axis of the implant for each patient. Gained bone width: the distance of bone profile between preoperative model and the three models, respectively, at 0, 2, and 4 mm apical to the platform of implant and perpendicular to the central axis of the implant for each patient. Abbreviation: CI, confidence interval.

## 7 | DIMENSIONAL ACCURACY EVALUATION

### 7.1 | Superimposition and contour deviation

The deviations among the contours of complete models, including CAD model, post-GBR model and post-implantation model of each case, were calculated by Materialize 3-matic. Maximum and minimum values represented the positive (over the contour of CAD model, or over the contour of GBR model when comparing post-GBR vs post-implantation) and negative (below the contour of CAD model, or below the contour of GBR model when comparing post-GBR vs post-implantation) distances respectively. Automatic analysis showed that the maximum deviations between post-GBR models, post-implantation models and CAD models were reached to 3.4 mm. Focused on the augmentation contour covered by 3D-PITMs, the descriptive analysis showed that the average deviation of minimum values from 16 cases between post-GBR, post-implantation models and CAD models respectively were  $-1.36 \pm 0.65$  and  $-1.72 \pm 0.92$  mm, and of maximum values were  $1.81 \pm 0.70$  and  $1.65 \pm 0.51$  mm (Table 2). The average deviation of minimum value between post-GBR and post-implantation models were  $-1.57 \pm 0.54$  mm, and of maximum values were  $1.36 \pm 0.54$  mm (Table 2). A further investigation was conducted in which all deviation values (whether positive or negative) were treated as the absolute values. The calculation showed that the mean absolute deviations among the augmentation contour of post-GBR contour, post-implantation contour and preoperative contour, respectively, were  $0.51 \pm 0.42$  and  $0.59 \pm 0.47$  mm, and that between the augmentation contour of post-GBR contour and post-implantation contour were  $0.39 \pm 0.33$  mm (Table 2).

### 7.2 | Deviation of augmented volume

Paired t test was conducted to compare the values of augmented bone volume between that in post-GBR models, post-implantation models (actual situation) and in CAD models (virtual plan). The average value of virtual augmented volume were lower than that in actual situation of post-GBR with the mean difference of  $-123.40 \pm 136.62$  mm<sup>3</sup> (95% CI:  $-196.20 \sim 50.60$  mm<sup>3</sup>), which showed a statistically significant difference ( $df = 15$ ,  $P = .003$ ). And that the average value of virtual augmented volume were slightly higher than that in actual situation of post-implantation with the mean difference of  $2.18 \pm 156.09$  mm<sup>3</sup> (95% CI:  $-80.99 \sim 85.36$  mm<sup>3</sup>), but no statistically significant difference was found ( $df = 15$ ,  $P = .956$ ) (Table 3).

### 7.3 | Deviation of augmented bone in 2D assessment

Compared with that in the CAD models, the horizontal augmentation of alveolar widths measured in cross-section views was relatively

**TABLE 4** Results of bone resorption

Volume changes (mm <sup>3</sup> )	Vertical resorption (mm)	Horizontal resorption (mm)		
		Mean ± SD (95% CI)	2 mm	4 mm
Mean ± SD (95% CI)	Mean ± SD (95% CI)	Mean ± SD (95% CI)		
–77.88 ± 44.23(46.24-0.9.53)	–0.09 ± 0.17(0.01-0.18)	–0.41 ± 0.27(0.27-0.55)	–0.34 ± 0.25(0.21-0.47)	–0.04 ± 0.51(–0.24-0.29)

Abbreviation: CI, confidence interval.

higher in the post-GBR and post-implantation models. The mean deviations in the post-GBR models presented of  $-0.33 \pm 1.39$  mm on the platform of implant,  $-0.42 \pm 1.09$  mm 2 mm apical to the platform, and  $-0.26 \pm 0.97$  mm 4 mm apically. And the mean deviations in the post-implantation models presented of  $-0.04 \pm 1.96$  mm on the platform of implant,  $-0.37 \pm 1.02$  mm, 2 mm apical to the platform, and  $-0.51 \pm 0.79$  mm, 4 mm apically. In contrast, the gained height of alveolar bone was higher in the CAD models than that in the post-GBR and post-implantation models, with the mean difference of  $0.22 \pm 1.00$  and  $0.56 \pm 1.35$  mm. The differences on the level of 4 mm apically in the post-implantation models had been found statistically significant ( $df = 15$ ,  $P < .05$ ) (Table 3).

## 8 | THE OUTCOMES OF BONE RESORPTION

After 10 to 18 months (average 13.3 years) follow-ups, all 16 augmentation sites showed stable bone volume with the volume changes of  $-77.88 \pm 44.23$  mm<sup>3</sup>. In vertical bone resorption, the average changes was  $-0.09 \pm 0.17$  mm (95% CI: 0.01-0.18 mm). In horizontal bone resorption, the average changes was  $0.41 \pm 0.27$  mm (95% CI: 0.27-0.55 mm) on the platform of the implants,  $0.34 \pm 0.25$  mm (95% CI: 0.21-0.47 mm) 2 mm apical to the platform and  $-0.04 \pm 0.51$  mm (95% CI:  $-0.24$  to 0.29 mm) 4 mm apically (Table 4).

## 9 | DISCUSSION

With the development of digital simulation technology and rapid prototyping manufacturing, 3D-PITM manufactured by the CAD/SLM techniques has proven to be a potential implant device in GBR treatment for atrophy alveolar bone.<sup>13,15,16,18,19,22,23</sup> In this study, 16 pieces of 3D-PITM were used in retrospective cases, presenting reliable effective of horizontal and/or vertical augmentation in bone defects of jaws. Moreover, a relative lower dehiscence rate (25%) was reported within the range of 0% to 33%, which were claimed by other authors in clinical studies of 3D-PITMs.<sup>16,18,19</sup> Coinciding with the previous reports, no severe adverse effect was found in the final results of bone augmentation.

Although CAD/SLM routine makes it possible to manufacture the customized Ti-mesh much more predictable according to individual bone morphology.<sup>20,22,24</sup> There was still a problem about whether or not the 3D-PITM could be applied to implement the precisely GBR in

line with the presurgical designs completely. Accurate bone augmentation can gain optimal bone volume not only for the implant placement, but also recover the facial contour of alveolar bone, which is necessary for esthetic restoration. Otherwise, excessive expansion of bone contour and extra bone grafting could be avoided.

Before the study, we observed clinically the deviation between the CAD planning and the final augmentation results. It may depend on the fitness of 3D-PITMs and dehiscence of soft tissue, which were both related to the clinical experience, the position accuracy of 3D-PITM and most probably the prototype of devices. In order to test the hypothesis above, this retrospective study was carried out, and it initially confirmed our concern about the accuracy problem.

In the superimposition analysis of 3D reconstruction models, the maximum deviations between the contours of post-GBR VS virtual and post-implantation VS virtual reached to 3.37 and 3.44 mm, respectively. Taken the contour of bone augmentation as a whole, the average difference of post-GBR model and post-implantation model was up to 1 mm approximately. According to comprehensive analysis of digital measurement in this study, three involved factors potentially influencing the accuracy of bone augmentation with 3D-PITMs have been initially proven.

Firstly, the precise placement of 3D-PITM is quite relevant to the accuracy of augmentation. Because of technique limitation, the contour of 3D-PITM cannot be separated but only can be mapped by the contour of bone graft mass in the interposition color maps. In 16 enrolled patients, apparent M-D (medial-distal) displacement ( $>2$  mm) of 3D-PITM might happened in three of post-GBR models compared with the virtual plan (Figure 4f,j,n), in B-P (buccal-palatal) direction it might occur in 3 patients ( $>1.5$  mm) (Figure 4g,i,k), while in C-A (crown-apical) direction it might occur in 5 patients ( $>1.5$  mm) (Figure 4b,c,d,h,m). In other words, 3D-PITMs might be positioned in the relatively accurate position for only four patients (25%). Although the prototype of 3D-PITMs were carefully designed, the installation and fixture were up to the surgical procedure. Placing the 3D-PITM on the defect sites with or without bone graft were quite different, since the sticky-bone mass filled onto the defects and meshes would, to certain extent hinder the correct position, and in consequence caused shifting or translocation. Meanwhile, efforts to correct the position by pulling the 3D-PITM might not be helpful, because the landmarks of position had been covered by the bone graft and the surgeon could only believe his/her own instinct. Besides, the stability of 3D-PITMs also matters. In the study of Seiler et al,<sup>18</sup> the loosening of mesh with or without infection of surgical area was found in eight patients, the rate of which was 7.8%. According to clinical evaluation,

no loosening of 3D-PITM had been found in these 16 patients, but we do have a case, which have not been enrolled into this study, suffering the exposure of mesh and subsequent infection because of the loosening of mesh.

Secondly, as many authors have reported, the so-called pseudo-periosteum (connective tissue layer) underneath Ti-mesh had been observed at every GBR sites, which may be a relevant factor for the accuracy of bone regeneration.<sup>9,21,25-27</sup> As a consequence of fibroblast invasion and micro-movement of the device, the pseudo-periosteum may occupy the osteogenesis space for 0 to 2 mm thickness in the clinical observation.<sup>26,28,29</sup> As described by Cucchi et al,<sup>26</sup> pseudo-periosteum was classified into three types: Type 1 (no tissue or tissue <1 mm); Type 2 (regular tissue between 1 and 2 mm); and Type 3 (irregular tissue or tissue >2 mm).<sup>26</sup> In the analysis of digital models in 16 cases, the thickness of new bone had been averagely reduced  $0.55 \pm 0.53$  mm comparing with the post-GBR models. Moreover, 68.75% of those patients ( $n = 16$ ) showed a type 1 pseudo-periosteum, 25% showed type 2, and 6.3% showed type 3. In addition, the difficulty of second stage resection of pseudo-periosteum may also lead to the loss of some new bone.<sup>27</sup> Until now, we cannot figure out a predictable way to prevent or reduce the invasion of the soft tissue, even if dual-membranes technique had been tried in many cases.<sup>19,30</sup> Therefore, it must be considered as a constant influence for volume deviation of bone in GBR combined with 3D-PITM. Correspondingly, we suggest 1.5 mm extended space over the planned contour of augmentation bone during the design of 3D-PITM.

Furthermore, the dehiscence of gingiva and Ti-mesh exposure may also reduce the bone gains underneath, and thus enhance the deviation in customized bone augmentation.<sup>18,31,32</sup> In this study, we compared not only the deviation of bone gain between the post-implantation models and the post-GBR models, but also the deviation difference between the 12 cases without complications and other 4 cases, which had suffered in dehiscence and exposure. As the exposures of 4 patients were all occurred on the crest of alveolar bone, the mean difference of  $0.62 \pm 0.62$  mm in gained bone height was found, higher than that of  $0.26 \pm 0.79$  mm in non-exposure group. The complication of four patients might be attribute to the difficulty in tension-free closure of mucoperiosteum flap. All of the four cases presented either severe vertical bone defects or expanding atrophy regions with over three missing teeth involved. By the way, the risky factor of 3D-PITM exposure may also lay on the over-stress onto the soft tissue, given by the labial muscle and the over-contour of the titanium devices.<sup>7,33</sup>

Beyond of the three factors above, the deviations might begin from the modeling of defects and the design of 3D-PITM. During the acquisition of the bone contour, the accuracy and resolution of CBCT scanning could be affected by so many factors, such as the minimal voxel (0.07-0.1 mm) of the CBCT system, the period of radiation exposure, and the motion of the patients.<sup>34</sup> However, the accuracy of CBCT data is not the only influencing factor of dimensional accuracy in defect modeling. Meanwhile, the software used for DICOM reconstruction and the range of threshold values could also have deep impact on it. In addition, multiple smoothing, stacking of digital 3D

model during the digital procedure might cause uncertain bone loss on the surface of the contour. As a whole, deviations in the modeling of the alveolar defect and neighbor bone volume might directly influence the final design of the 3D-PITM, and then reduce the accuracy of the device position.

Now, we could make it clear that only precisely SLM manufacture of devices ( $193 \mu\text{m}$  as the mean error) may not assure the accurate position of 3D-PITM, nor the committed bone augmentation volume in final. In order to improve the dimensional accuracy of bone augmentation with 3D-printing individualized Ti-mesh, the following suggestions need to be considered.

1. Higher resolution of CBCT scanning is helpful to obtain accurate data of alveolar bone, which means a lot for the virtual design of 3D-PITM.
2. During the modeling of virtual bone defect, CT threshold is the critical variable for the final look of 3D models' contour.
3. Auxiliary template for preparation of screws fixture is recommend. It could be designed and manufactured by means of CAD-CAM, and might help the correct installation of 3D-PITM.
4. Appropriate number and sites of fixture screws is critical for better stability of 3D-PITM sitting on the alveolar crest and over the bone grafting material.
5. Experience surgical skill and proper handling of complications are needed to prevent the negative influence of bone augmentation.<sup>17</sup>

In addition, appropriate soft tissue management is of paramount importance to avoid complications and increase the success of bone augmentation therapy.<sup>35,36</sup> This includes the planning of the incision,<sup>37</sup> adequate flap design, and a tension-free primary wound closure.<sup>18</sup> The incision and flap design includes a poncho flap with a deep vestibular incision, a full flap with a midcrestal ridge incision, a split-thickness flap, a rotation flap, or the tunnel technique. However, as reported by Seiler, different surgical access did not show significant association with the prevalence of dehiscence.<sup>18</sup> In most studies, a tension-free closure of wound is considered as an important factor in avoiding exposure of Ti-mesh.<sup>19,36,38</sup> Therefore, two vertical incision one to three teeth away from the edentulous region and a periosteal releasing incision were reported to reducing the tension of flap. And modified horizontal mattress suture, vertical mattress suture, and single sutures were also suggested to gain a connective tissue to connective tissue contact. In the last decade, PRF matrix has been widely used to cover Ti mesh, and has been proven to accelerate the healing process of soft tissues and prevent complications of Ti-mesh.<sup>30,36,39</sup> In the study of Ghanaati et al, a new avenue using solid PRF matrix to cover the gap between the approximated flap margins in terms of open healing was presented, and it showed satisfactory clinical and histological outcomes.<sup>17</sup> In our study, we also suggested this method in following situations: severe bone defects; defects with more than three teeth loss or surgeons who are lack of surgical experience with regard to achieve a tension-free closure. Besides, surgical splints were also reported to provide a better wound healing although no statistically significant.<sup>36</sup>

Limited studies specially reported bone stability with Ti-mesh. Zhang et al<sup>38</sup> evaluated the labial bone resorption using CBCT, the results showed that the median resorption after average 23.13 months for the vertical dimension was  $-0.81 \pm 1.00$  mm and the horizontal alteration measured at the top of the implants was  $0.13 \pm 1.19$  mm. The resorption values evaluated in our study seemed to be more positive. The bone resorption in vertical dimension was  $-0.09 \pm 0.17$  mm, and for horizontal dimension, the average changes was  $0.41 \pm 0.27$ ,  $0.34 \pm 0.25$ , and  $-0.04 \pm 0.51$  mm at 0, 2, and 4 mm apical to the platform of implant. Reasonably, the support and protection of 3D-PTIM had assured the quality of bone formation beneath. Meanwhile, the time of follow-up was short, the volume and contours of the regenerated bone should ongoing change during the remodeling processes.<sup>5,38</sup>

In the end, we must admit that the limitation of the present study was apparent. First of all, it was a small-sampled retrospective study without a control group, and the sample size was inhomogeneous, most of which located in the premaxilla. Second, the time of follow-up was only 10 to 18 months after the implant placement in this study, but we will continue following and recording the prognosis of bone reconstruction. However, the long-term stability and peri-implant recession of soft and hard tissue in cases of customized GBR with 3D-PITM were not the primary objects of this study.

In the end, we must admit the limitation of the present study is related to the small number of sample and inhomogeneous sample size, most of which located in the premaxilla. This is due to the application of 3D-PITM for bone augmentation was still in the preliminary-stage of clinical practice, and a lot of patients have not yet reached the time to remove the Ti-mesh. In addition, the time of follow-up was a little short, even the long-term stability and peri-implant recession of soft and hard tissue in cases of customized GBR with 3D-PITM were not the primary objects of this study. Even though the augmentation accuracy with 3D-PITM could be initially evaluated, a prospective controlled study with a larger sample followed for a longer period of time are needed.

## 10 | CONCLUSION

In conclusion, the dimensional accuracy evaluation of customized bone grafting has positive significance for the application of 3D-PITM, but the deviation of the dimensional accuracy was still a little high. To improve the dimensional accuracy of customized bone grafting, it is necessary to further optimize preoperative design and surgical techniques.

## ACKNOWLEDGMENTS

This work was supported by grants from the National Science Foundation of China (Grant nos. 11872135, 12072055, and 31100690), the Chongqing Science and Technology Bureau's new high-end R&D institution (Grant no. CSTC2018(C)XXYFJG0004), the Project Supported by Program for Innovation Team Building at institutions of Higher Education in Chongqing in 2016 (Grant

no. CXTDG201602006). The authors would like to gratefully acknowledge Reborn Medical Technology Co., Ltd., Shanghai, China, for the manufacture of 3D-printing individual Ti-mesh and Dr. Lingling Zheng, Dr. Hui Gao for their assistance in computer aided design of 3D-printing individual Ti-mesh.

## CONFLICT OF INTEREST

No conflicts of interest related to this study.

## DATA AVAILABILITY STATEMENT

The data that support the findings of this study are available on request from the corresponding author. The data are not publicly available due to privacy or ethical restrictions.

## ORCID

Yuanding Huang  <https://orcid.org/0000-0003-4517-3901>

## REFERENCES

1. Draenert FG, Huetzen D, Neff A, Mueller WE. Vertical bone augmentation procedures: basics and techniques in dental implantology. *J Biomed Mater Res A*. 2014;102:1605-1613.
2. Esposito M, Grusovin MG, Felice P, Karatzopoulos G, VVorthington H, Coulthard P. Interventions for replacing missing teeth: horizontal and vertical bone augmentation techniques for dental implant treatment. *Cochrane Database Syst Rev*. 2009;4(4):CD003607.
3. Benic GI, Hämmerle HFC. Horizontal bone augmentation by means of guided bone regeneration. *Periodontol* 2000. 2014;66:13-40.
4. Urban IA, Nagursky H, Lozada JL, Nagy K. Horizontal ridge augmentation with a collagen membrane and a combination of particulated autogenous bone and anorganic bovine bone-derived mineral: a prospective case series in 25 patients. *Int J Periodontics Restorative Dent*. 2013;33:299-307.
5. Basler T, Naenni N, Schneider D, Hammerle CHF, Jung RE, Thoma DS. Randomized controlled clinical study assessing two membranes for guided bone regeneration of peri-implant bone defects: 3-year results. *Clin Oral Implants Res*. 2018;29:499-507.
6. Rakhmatia YD, Ayukawa Y, Furuhashi A, Koyano K. Current barrier membranes: titanium mesh and other membranes for guided bone regeneration in dental applications. *J Prosthodont Res*. 2013;57:3-14.
7. Jiang X, Zhang Y, Di P, Lin Y. Hard tissue volume stability of guided bone regeneration during the healing stage in the anterior maxilla: a clinical and radiographic study. *Clin Implant Dent Relat Res*. 2018;20:68-75.
8. Soldatos NK, Stylianou P, Koidou VP, Angelov N, Yukna R, Romanos GE. Limitations and options using resorbable versus non-resorbable membranes for successful guided bone regeneration. *Quintessence Int*. 2017;48:131-147.
9. Briguglio F, Falcomata D, Marconcini S, Fiorillo L, Briguglio R, Farronato D. The use of titanium mesh in guided bone regeneration: a systematic review. *Int J Dent*. 2019;2019:9065423.
10. Rasia-dal Polo M, Poli PP, Rancitelli D, Beretta M, Maiorana C. Alveolar ridge reconstruction with titanium meshes: a systematic review of the literature. *Med Oral Patol Oral Cir Bucal*. 2014;19:e639-e646.
11. Louis PJ, Gutta R, Said-Al-Naief N, Bartolucci AA. Reconstruction of the maxilla and mandible with particulate bone graft and titanium mesh for implant placement. *J Oral Maxillofac Surg*. 2008;66:235-245.
12. Arx TV, Kurt B. Implant placement and simultaneous ridge augmentation using autogenous bone and a micro titanium mesh: a prospective clinical study with 20 implants. *Clin Oral Implants Res*. 1999;10:24-33.
13. Cicocca L, Crescenzo MFFD, Corinaldes G, Scotti R. Direct metal laser sintering (DMLS) of a customized titanium mesh for

- prosthetically guided bone regeneration of atrophic maxillary arches. *Med Biol Eng Comput.* 2011;49:1347-1352.
14. Wang H, Su K, Su L, Liang P, Ji P, Wang C. The effect of 3D-printed Ti6Al4V scaffolds with various macropore structures on osteointegration and osteogenesis: a biomechanical evaluation. *J Mech Behav Biomed Mater.* 2018;88:488-496.
  15. Bai L, Ji P, Li X, Gao H, Li L, Wang C. Mechanical characterization of 3D-printed individualized Ti-mesh (membrane) for alveolar bone defects. *J Healthc Eng* 2019; 2019: 4231872, 1, 13.
  16. Sumida T, Otawa N, Kamata YU, et al. Custom-made titanium devices as membranes for bone augmentation in implant treatment: clinical application and the comparison with conventional titanium mesh. *J Craniomaxillofac Surg.* 2015;43:2183-2188.
  17. Ghanaati S, Al-Maawi S, Conrad T, Lorenz J, Rossler R, Sader R. Bio-material-based bone regeneration and soft tissue management of the individualized 3D-titanium mesh: an alternative concept to autologous transplantation and flap mobilization. *J Craniomaxillofac Surg.* 2019;47:1633-1644.
  18. Seiler M, Peetz M, Witkowskia R. Individualized CAD-CAM-produced titanium scaffolds for alveolar bone augmentation: a retrospective analysis of dehiscence events in relation to demographic and surgical parameters. *J Oral Sci Rehab.* 2018;4:38-46.
  19. Sagheb K, Schiegnitz E, Moergel M, Walter C, Al-Nawas B, Wagner W. Clinical outcome of alveolar ridge augmentation with individualized CAD-CAM-produced titanium mesh. *Int J Implant Dent.* 2017;3:36.
  20. Otawa N, Sumida T, Kitagaki H, et al. Custom-made titanium devices as membranes for bone augmentation in implant treatment: modeling accuracy of titanium products constructed with selective laser melting. *Craniomaxillofacial Surg.* 2015;43:1289-1295.
  21. Boyne P, Cole M, Stringer D, Shafqat J. A technique for osseous restoration of deficient edentulous maxillary ridges. *J Oral Maxillofacial Surg.* 1985;43:87-91.
  22. Inoue K, Nakajima Y, Omori M, et al. Reconstruction of the alveolar bone using bone augmentation with selective laser melting titanium mesh sheet a report of 2 cases. *Implant Dent.* 2018;27:602-607.
  23. Ciocca L, Lizio G, Baldissara P, Sambuco A, Scotti R, Corinaldesi G. Prosthetically CAD-CAM-guided bone augmentation of atrophic jaws using customized titanium mesh: preliminary results of an open prospective study. *J Oral Implantol.* 2018;44:131-137.
  24. Silva DN, MGd O, Meurer E, Meurer MI, JVLd S, Santa-Bárbara A. Dimensional error in selective laser sintering and 3D-printing of models for craniomaxillary anatomy reconstruction. *J Craniomaxillofac Surg.* 2008;36:443-449.
  25. Gerardo P, Giuseppe L, Giuseppe C, Claudio M. Titanium mesh technique in rehabilitation of totally edentulous atrophic maxillae: a retrospective case series. *J Periodontol.* 2016;87:519-528.
  26. Cucchi A, Sartori M, Aldini NN, Vignudelli E, Corinaldesi G. A proposal of pseudo-periosteum classification after GBR by means of titanium-reinforced d-PTFE membranes or titanium meshes plus cross-linked collagen membranes. *Int J Periodontics Restorative Dent.* 2019;39: e157-e165.
  27. Atef M, Tarek A, Shaheen M, Alarawi RM, Askar N. Horizontal ridge augmentation using native collagen membrane vs titanium mesh in atrophic maxillary ridges: randomized clinical trial. *Clin Implant Dent Relat Res.* 2020;22:156-166.
  28. Rakhmatia YD, Ayukawa Y, Atsuta I, Furuhashi A, Koyano K. Fibroblast attachment onto novel titanium mesh membranes for guided bone regeneration. *Odontology.* 2015;103:218-226.
  29. Gutta R, Baker RA, Bartolucci AA, Louis PJ. Barrier membranes used for ridge augmentation: is there an optimal pore size? *J Oral Maxillofac Surg.* 2009;67:1218-1225.
  30. Lorenz J, Al-Maawi S, Sader R, Ghanaati S. Individualized titanium mesh combined with platelet-rich fibrin and Deproteinized bovine bone: a new approach for challenging augmentation. *J Oral Implantol.* 2018;44:345-351.
  31. Miyamoto I, Funaki K, Yamauchi K, Kodama T, Takahashi T. Alveolar ridge reconstruction with titanium mesh and autogenous particulate bone graft: computed tomography-based evaluations of augmented bone quality and quantity. *Clin Implant Dentistry Related Res.* 2011;14:304-311.
  32. Hamzani Y, Chaushu G. Evaluation of early wound healing scales/indexes in oral surgery: a literature review. *Clin Implant Dent Relat Res.* 2018;20:1030-1035.
  33. Jiang X, Zhang Y, Chen B, Lin Y. Pressure bearing device affects extraction socket remodeling of maxillary anterior tooth. A prospective clinical trial. *Clin Implant Dent Relat Res.* 2017;19:296-305.
  34. Fokas G, Vaughn VM, Scarfe WC, Bornstein MM. Accuracy of linear measurements on CBCT images related to presurgical implant treatment planning: a systematic review. *Clin Oral Implants Res.* 2018;29 (Suppl 16):393-415.
  35. Lim G, Lin GH, Monje A, Chan HL, Wang HL. Wound healing complications following guided bone regeneration for ridge augmentation: a systematic review and meta-analysis. *Int J Oral Maxillofac Implants.* 2018;33:41-50.
  36. Hartmann A, Seiler M. Minimizing risk of customized titanium mesh exposures—a retrospective analysis. *BMC Oral Health.* 2020;20:36.
  37. Kleinheinz J, Buchter A, Kruse-Losler B, Weingart D, Joos U. Incision design in implant dentistry based on vascularization of the mucosa. *Clin Oral Implants Res.* 2005;16:518-523.
  38. Zhang T, Zhang T, Cai X. The application of a newly designed L-shaped titanium mesh for GBR with simultaneous implant placement in the esthetic zone: a retrospective case series study. *Clin Implant Dent Relat Res.* 2019;21:862-872.
  39. Torres J, Tamimi F, Alkhraisat MH, et al. Platelet-rich plasma may prevent titanium-mesh exposure in alveolar ridge augmentation with anorganic bovine bone. *J Clin Periodontol.* 2010;37:943-951.

**How to cite this article:** Li L, Wang C, Li X, Fu G, Chen D, Huang Y. Research on the dimensional accuracy of customized bone augmentation combined with 3D-printing individualized titanium mesh: A retrospective case series study. *Clin Implant Dent Relat Res.* 2021;23:5–18. <https://doi.org/10.1111/cid.12966>